EPSC Abstracts
Vol. 9, EPSC2014-602-6, 2014
European Planetary Science Congress 2014

Automatic Crater Detection and Implications for Surface Age Estimation

Atheer L. Salih[1], A. Boukercha[1], A. Grumpe[1], C. Wöhler[1], H. Hiesinger[2]
[1]Image Analysis Group, TU Dortmund University, D-44227 Dortmund, Germany; atheer.altameemi@tu-dortmund.de
[2]Institut für Planetologie, Westfälische Wilhelms-Universität Münster, D-48149 Münster, Germany

1. Introduction

Crater size-distribution measurements (CFSDs) are an important tool for the assessment of the ages of surface regions [1,2]. The freely available software Craterstats2 [3] allows for the determination of the absolute model ages (AMA) of the surface if the number and diameters of the craters within the count area of a certain size are known. In this context, manual counting and measuring of craters is a time-consuming process while automatic crater detection may lead to increased false positive detections, missed craters and possibly inaccurate diameter determination. However, the influence of such recognition errors of automated crater detection systems on the estimated model age has not yet been fully investigated. Current automatic crater detection algorithms depend on either optical images or digital elevation models (DEM) [4]. In this study, we compare different crater detectors and their behaviour in the context of surface age determination.

2. Methodology

The lunar crater catalogue LU78287GT [5] contains a list of manually verified craters detected with the algorithm described in [4,5] We apply the photometric surface refinement method in [6] and the DEM-based detector described in [4] and extended in [5] to detect possible craters. Additionally, the intensity image based detector described in [7] is applied to the image to derive a different set of automatically detected craters. Finally, the two-stage method [8] is applied to obtain a third set of craters.

Based on the LU78287GT catalogue, a reference model age is determined for a calibration region, and the detection thresholds of the automatic methods are adapted such that their estimated model ages are as similar as possible to that of the reference model age for all three methods. Afterwards, all crater detection methods are applied to a different region of interest, and the corresponding surface ages are derived and compared.

The LU78287GT catalogue contains the craters visible in a part of Moon Mineralogy Mapper (M^3) image M3G20090205T193313. From this large area, parts of the floors of the large impact craters Ptolemaeus and Alphonsus were extracted, where the floor of Ptolemaeus serves as the calibration region and the floor of Alphonsus as the region of interest, whose model age is estimated using the different automatic crater detection approaches. The craters detected with the different methods are shown in Figs. 1 and 3. In these two regions, the surface is illuminated at incidence angles between about 52° and 53°.

3. Results

The age estimates of the three automatic crater detection approaches adjusted to those obtained for the ground truth catalogue are shown for the calibration area on the floor of Ptolemaeus crater in Fig. 2. As intended for calibration, all four model ages are identical. The isochrons were fitted to the crater diameter interval 0.7–2.5 km.

The detection thresholds obtained by the calibration procedure were retained when applying the automatic detection methods to the region on the floor of Alphonsus crater (Fig. 3). The estimated model ages inferred from the automatic detection results are between 3.69 and 3.82 Ga, which compares well with the model age of 3.76 Ga obtained based on the LU78287GT catalogue (Fig. 4).

4. Conclusion

The results show that the estimation of surface ages based on automatic crater detection may yield realistic results when an appropriate calibration procedure is applied.

References

[1] Neukum, G. (1983) *Meteoritenbombardement und Datierung planetarer Oberflächen.* Univ. of Munich.

[2] Michael, G. G. and Neukum G. (2010) *Planetary surface dating from crater size-frequency distribution measurements: Partial resurfacing events and statistical age uncertainty.* Earth and Planetary Science Letters 294(3-4), 223-229.

[3] Michael, G. (2014) *Craterstats.* http://hrscview.fu-berlin.de/craterstats.html. Accessed: 2014/05/02.

[4] Salamuničcar, G. and Lončarić, S. (2010) *Method for Crater Detection From Martian Digital Topography Data Using Gradient Value/Orientation, Morphometry, Vote Analysis, Slip Tuning, and Calibration.* IEEE Trans. Geoscience and Remote Sensing 48(5), 2317-2329.

[5] Salamuničcar, G. et al. (2013) *Hybrid method for crater detection based on topography reconstruction from optical images and the new LU78287GT catalogue of Lunar impact craters.* Adv. Space Research 53(12), 1783-1797.

[6] Grumpe, A. et al. (2013) *Construction of lunar DEMs based on reflectance modelling.* Adv. Space Research 53(12), 1735-1767.

[7] Grumpe, A. and Wöhler, C. (2013) *Generative Template-based Approach to the Automated Detection of Small Craters*. EPSC Abstracts 8, EPSC2013-685.

[8] Boukercha, A. et al. (2014) *Automatic Crater Recognition using Machine Learning with Different Features and their Combinations.* LPSC XXXXV, Abstract #2842.

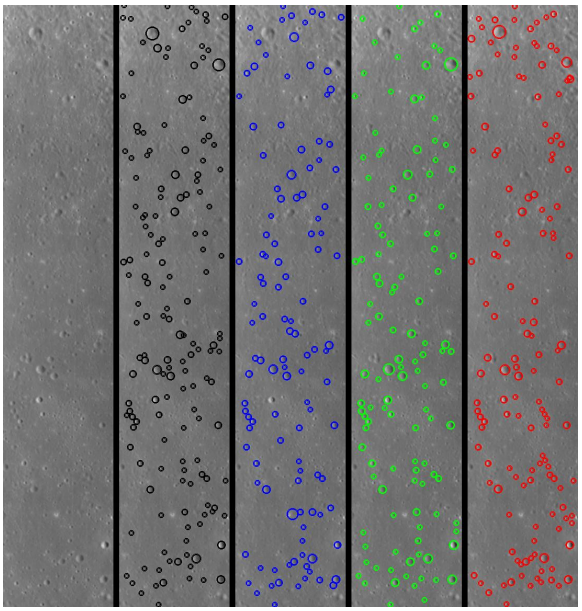

Figure 1: Detected craters within Ptolemaeus crater. Black: LU78287GT [5]. Blue: DEM-based detector [4,5]. Green: image-based detector [7]. Red: two-stage method [8].

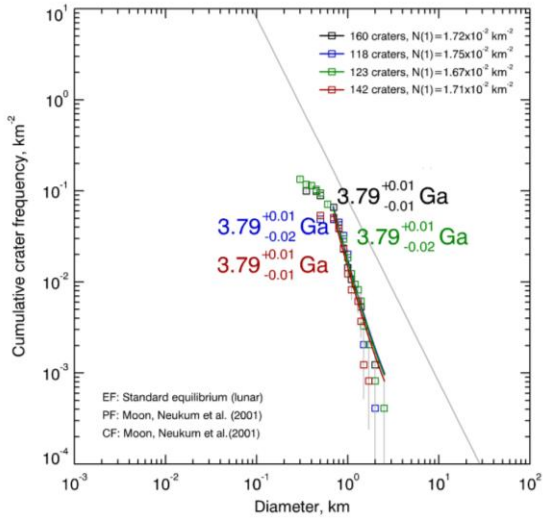

Figure 2: Derived model ages for the region of interest on the floor of Ptolemaeus crater. Colours as in Fig. 1.

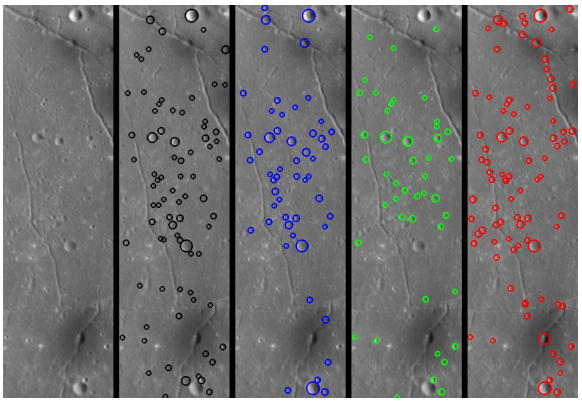

Figure 3: Detected craters within Alphonsus crater. Colours as in Fig. 1.

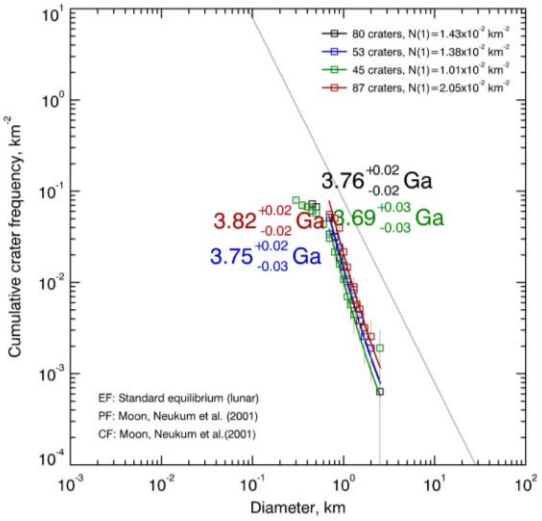

Figure 4: Derived model ages for the region of interest on the floor of Alphonsus crater. Colours as in Fig. 1.